JOURNAL OF MAGNETIC RESONANCE **132,** 287–297 (1998)
ARTICLE NO. MN981389

A Pulsed Field Gradient NMR Technique for the Determination of the Structure of Suspensions of Non-Brownian Particles with Application to Packings of Spheres

L. Talini, J. Leblond, and F. Feuillebois

Laboratoire de Physique et Mécanique des Milieux Hétérogènes, URA 857 au CNRS, ESPCI, 10 rue Vauquelin, 75231 Paris Cedex 05, France

E-mail: talini@pmmh.espci.fr

Received July 18, 1997

The internal structure of systems of particles in a liquid is studied with a novel NMR technique based on the measurement of the squared modulus of the magnetization in presence of a pulsed field gradient. The formalism is analogous to the one used in classical scattering techniques (light, X-rays, neutrons); it allows similar information to be obtained about the structure (in particular, the structure factor $S(\mathbf{q})$). The main improvement is that the range of particles sizes is 10 μm to 1 mm, as compared with the range of the scattering techniques ($<$5 μm). The NMR technique was validated by studying packings of spherical particles of mean diameter 240 μm created by sedimentation. The profile of the experimental squared modulus of the magnetization versus the wave vector provides results for the mean size of particles and the compacity. The main feature is that it depends on the pair distribution function, and the present results are in good agreement with a model based on the Percus–Yevick approximation. This technique is then particularly adapted to systems such as non-Brownian suspensions, fluidized beds, porous media, and sediments.

INTRODUCTION

The techniques of light scattering, small-angle X-ray scattering, and small-angle neutron scattering are currently used to characterize colloidal systems. These techniques are useful to determine the size of dispersed particles in a solvent and the structure of a colloidal system through the pair correlation function $1 - g(r)$, where $g(r)$ is the pair distribution function defined as the density of probability to find a couple of particles separated by a distance r. However, all three techniques have limited ranges of application (*1–3*), the accessible length scales being related to the range of values of the scattering wave vector which can be scanned (10^{-2} Å^{-1} $< q <$ 2 Å^{-1} by X-ray scattering; 10^{-3} Å^{-1} $< q <$ 2 Å^{-1} by neutron scattering; 2×10^{-5} Å^{-1} $< \mathrm{q} < 2 \times 10^{-3}$ Å^{-1} by light scattering). These techniques are thus adapted to systems with particles of small size, the maximum being 5 μm in the case of the light scattering method. They are inefficient for systems with a larger characteristic size such as non-Brownian suspensions, porous media, and fluidized beds. In this paper, we show that information about the structure of systems with a characteristic size larger than 10 μm can be gained with NMR, the pair correlation function being derived with a formalism analogous to the classical scattering techniques.

The pulsed field gradient spin-echo (PFGSE) NMR technique has been used for many years to study diffusion and flow in porous media. This method provides information about the microstructure in the host material when boundaries hinder normal diffusive transport (*4*). Recent works point out that the distribution of probability of the molecular displacements $P(\Delta z, t)$, along the z axis, during an interval of time t, can be obtained using the PFGSE sequence; the echo signal M_1 being a function of the intensity of the field gradient $\mathbf{G}$, the probability $P(\Delta z, t)$ then appears as the Fourier transform of $M_1(\mathbf{G})$. This technique has been introduced by K. Fukuda and A. Hirai (*5*) in order to find the axial distribution of probability of velocity in a liquid flowing in a cylindrical channel, then by J. Kärger and W. Heink (*6*) to study the n-hexane diffusion in a loose assemblage of NaX zeolite crystallites. The analogy between NMR in the presence of a pulsed field gradient and diffraction was pointed out by P. Mansfield and P. K. Grannel (*7*) in the context of NMR imaging. More recently, diffraction-like effects in PFGSE experiments have been discussed for the diffusion both in connected structures (*8*) and in impermeable structures (*9*). It was also demonstrated by D. G. Cory and N. Garroway (*9*) that when boundaries hinder normal diffusive transport of the particles, the distribution of displacements $P(\Delta z, t)$ then approaches the fluid density autocorrelation function in the container for large values of the duration t of the NMR sequence. Thus, in the case of restricted motion in an enclosed pore, PFGSE experiments are

1090-7807/98 $25.00

mathematically similar to the experiments of optical diffraction through a single slot. P. T. Callaghan *et al.* (*10*) have independently developed this analogy for porous media with connected pores, in which a spin-bearing molecule originating in one pore can migrate to other pores. Provided the time scale for the diffusion within pores is much shorter than for the diffusion between pores, $P(\Delta z, t)$ becomes the product of the pore density by the probability of jumps between pores; in an assembly of monodisperse polystyrene spheres where the pore spacing is roughly equal to the sphere diameter (18.8 μm), the PFGSE–NMR experiments are used to obtain by a Fourier transform the ''image'' of the pore autocorrelation function convoluted with diffusion-weighted three-dimensional lattice correlation function. In a recent work, G. A. Barral *et al.* (*11*) have used NMR imaging to obtain the density autocorrelation function in structural materials. For NMR imaging, the spatial information is encoded by applying a magnetic gradient field $\mathbf{G}$ during a time t. A particle situated at a position $\mathbf{r}$ then induces a phase shift $\mathbf{k}\cdot\mathbf{r}$, $\mathbf{k}$ being the wave vector defined as

$$\mathbf{k} = \gamma \cdot \mathbf{G} \cdot t, \qquad [1]$$

where γ is the gyromagnetic ratio for the proton.

The volumic density of nuclei $\rho(\mathbf{r})$ is extracted by a Fourier transform of the signal $M(\mathbf{k})$ considered as a function in $\mathbf{k}$-space. Applying the Wierner–Khintchin theorem, the authors have shown that the density autocorrelation function is related to $M(\mathbf{k})$ by

$$\langle \rho(\mathbf{r}) \cdot \rho(\mathbf{r} + \Delta\mathbf{r}) \rangle = \frac{1}{(2\pi)^3 V} \int |M(\mathbf{k})|^2 e^{i\mathbf{k}\cdot\Delta r} d\mathbf{k}, \qquad [2]$$

where V is the measurement volume and $\langle\ \rangle$ denotes an average over all possible positions within the sample volume V. By definition, $\langle \rho(\mathbf{r}) \cdot \rho(\mathbf{r} + \Delta\mathbf{r}) \rangle$ is the Patterson function, which is characteristic of the structure. This concept was applied to the study of nylon monofilament fibers packed in glass tubes filled up with water, the fibers being in a vertical position. Using a slice NMR imaging technique, Barral *et al.* obtain the Patterson function of the image of a radial slice of the fibers by measuring the modulus of the signal.

In this paper, we show that systems with particles of any shape, possibly in motion, can be studied by NMR in presence of a pulsed field gradient. The formalism being similar to one of the classical scattering methods, we can obtain information about the size and shape of particles, and about the structure of the system through the pair distribution function. It is shown in the first section how this function can be obtained by studying the squared modulus of the signal. The presentation is specialized here to the case of spherical particles. We then consider in the second section the particular case of a homogeneous suspension. The technique is applied to packings of spheres created by sedimentation. The experimental procedure and results are then presented in the third section. The experimental result for the pair distribution function is compared to the one obtained by the Percus–Yevick theory in the fourth section.

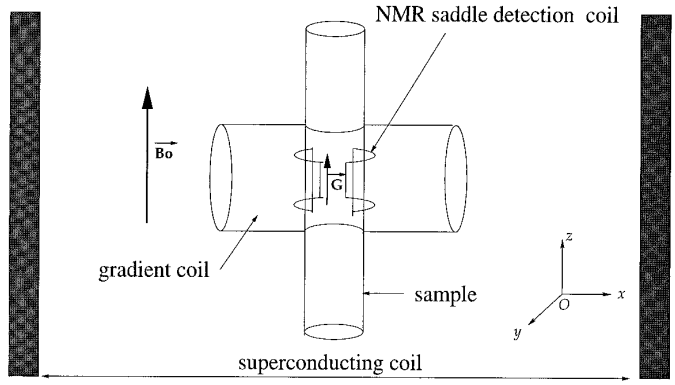

FIG. 1. Measurement zone of the spectrometer.

MAGNETIZATION OF A SUSPENSION IN A PULSED FIELD GRADIENT

Consider a suspension of particles in a liquid rich in protons. When a magnetic field is applied to the suspension, the main resulting magnetization is that of the liquid. The following formulation is valid for particles of any shape but will later be specialized to spheres.

A simplified representation of the spectrometer is shown in Fig. 1. The sample is placed in a vertical tube of diameter $D = 1$ cm. A superconducting coil creates a vertical magnetic field $B_0 = 2.35$ T and induces a macroscopic magnetization in the sample. In the center of this coil, an NMR saddle coil is placed around the tube to deliver radiofrequency pulses at the resonance frequency of protons and to detect the magnetization. The saddle coil influences the volume $V = 0.5$ cm^3 of a cylinder of radius $r = 0.4$ cm and height $h = 1$ cm which defines the measurement zone. The gradient field pulses are provided by a quadrupole gradient coil perpendicular to the tube that generates a vertical pulsed field gradient $\mathbf{G}$ of up to 0.88 T/m. The NMR sequence is described in Fig. 2. At an initial time t_i, an impulse tilts the magnetization onto the horizontal plane in the direction of the x axis. It is followed by a constant pulsed gradient field. The signal detected in the radiofrequency coil immediately after the instant t_i is proportional to the magnetization inside the coil. $\rho(\mathbf{r}, t_i)$ is the spin density of protons in the suspension at time t_i, and $f(\mathbf{r})$ the apparatus function which describes the sensibility map of the radiofrequency coil. This function is

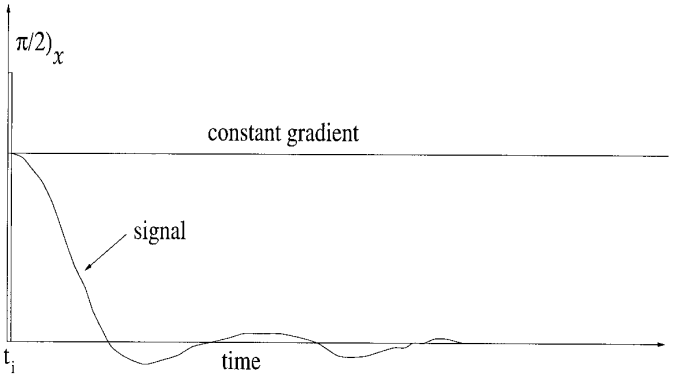

FIG. 2. NMR sequence considered for the calculation includes a $\pi/2$ impulsion and a constant field gradient simultaneously.

normalized so the maximum value is 1. The expression for the magnetization of the measurement zone at time t_i then is

$$M(t_i) = \int_E \rho(\mathbf{r}, t_i) f(\mathbf{r}) d\mathbf{r}, \qquad [3]$$

where E is the whole space.

When a pulsed field gradient $\mathbf{G}$ is applied starting from time t_i, the magnetization at time $t_i + t$ is (*8*)

$$M(\mathbf{k}, t_i) = \int_E \rho(\mathbf{r}, t_i) f(\mathbf{r}) e^{i \cdot \mathbf{k} \cdot \mathbf{r}} d\mathbf{r}. \qquad [4]$$

The movements of protons during t are thereby neglected, and the wave vector $\mathbf{k} = \gamma \cdot \mathbf{G} \cdot t$ is introduced, where γ is the gyromagnetic constant of the proton. The magnetization appears in Eq. [4] as the Fourier transform of the product of the spin density and the apparatus function. There is here an analogy with the techniques of light, neutron, and X-ray scattering in which the scattered amplitude appears as the Fourier transform of the volumic polarizability, density of scattering length, and density of electrons, respectively [see, e.g., (*1*), (*2*), (*3*)]. These classical techniques give information about the structure of dispersed media by studying the squared modulus of the scattered amplitude. In a similar way, the squared modulus of the magnetization may provide a characterization technique for the structure of the suspension. For this purpose, we first calculate the magnetization due to an ensemble of particles in a liquid.

Assuming that the protons are only in the liquid, the proton spin density of the suspension is

$$\rho(\mathbf{r}, t_i) = \rho_0 \left(1 - \sum_{j=1}^{N} h_j(\mathbf{r} - \mathbf{r_j}, t_i) \right), \qquad [5]$$

where ρ_0 is the spin density of particle-free liquid, and $h_j(\mathbf{r} - \mathbf{r_j})$ is a characteristic function defined as

$$\begin{cases} h_j(\mathbf{r} - \mathbf{r_j}, t_i) = 0 \\ \quad \text{if } \mathbf{r} \text{ corresponds to a point in the liquid} \\ h_j(\mathbf{r} - \mathbf{r_j}, t_i) = 1 \\ \quad \text{if } \mathbf{r} \text{ corresponds to a point in a particle.} \end{cases}$$

We can remark that h_j depends on the shape of particles and is therefore different for each particle in the most general case.

By substituting the spin density given by Eq. [5] into Eq. [4], we obtain

$$M(\mathbf{k}, t_i) = \rho_0 (\tilde{f}(\mathbf{k}) - M_S(\mathbf{k}, t_i)), \qquad [7]$$

where $\tilde{f}(\mathbf{k})$ is the Fourier transform of the apparatus function:

$$\tilde{f}(\mathbf{k}) = \int_E f(\mathbf{r}) e^{i \cdot \mathbf{k} \cdot \mathbf{r}} d\mathbf{r} \qquad [8]$$

and $M_S(\mathbf{k}, t_i)$, with $\mathbf{r}' = \mathbf{r} - \mathbf{r_j}$, is given by

$$M_S(\mathbf{k}, t_i) = \sum_{j=1}^{N} e^{i \cdot \mathbf{k} \cdot \mathbf{r} j} \int_E f(\mathbf{r}' + \mathbf{r_j}) h(\mathbf{r}', t_i) e^{i \cdot \mathbf{k} \cdot \mathbf{r}'} d\mathbf{r}'. \qquad [9]$$

In the integral of the previous equation, the function $h(\mathbf{r}, t_i)$ is nonzero inside the volume v_j of particle j; hence, the integration is reduced to the volume v_j. However, since v_j is much smaller than the measurement volume V, the apparatus function defining V may be taken as constant in v_j, which yields

$$f(\mathbf{r}' + \mathbf{r_j}) = \mathrm{f}(\mathbf{r_j}). \qquad [10]$$

Using this expression, the magnetization can be written as

$$M(\mathbf{k}, t_i) = \rho_0 \tilde{f}(\mathbf{k}) - \rho_0 \sum_{j=1}^{N} v_j \tilde{F}(\mathbf{k}, j) e^{i \cdot \mathbf{k} \cdot \mathbf{r}_j} f(\mathbf{r_j}), \qquad [11]$$

where $v_j \tilde{F}(\mathbf{k}, j)$ is the Fourier transform of $h_j(\mathbf{r}, t_i)$:

$$v_j \tilde{F}(\mathbf{k}, j) = \int_E h_j(\mathbf{r}) e^{i \cdot \mathbf{k} \cdot \mathbf{r}} d\mathbf{r}. \qquad [12]$$

Henceforth, $\tilde{F}(\mathbf{k}, j)$ is called the form factor of particle j. We shall now simplify the calculation by considering spherical

particles of the same size. The form factor has then a classical form well known in the light scattering literature:

$$\tilde{F}(kR) = 3\,\frac{\sin kR - kR\cos kR}{(kR)^3}, \qquad [13]$$

where R is the radius of spheres and k the modulus of the wave vector $\mathbf{k}$. The expression for the magnetization of a monodisperse suspension of spherical particles is eventually

$$M(\mathbf{k}, t_i) = \rho_0 \tilde{f}(\mathbf{k}) - \rho_0 v \tilde{F}(kR) \sum_{j=1}^{N} e^{i\cdot\mathbf{k}\cdot\mathbf{r}_j} f(\mathbf{r_j}). \qquad [14]$$

Squaring the modulus of the magnetization in Eq. [14], we obtain

$$\begin{aligned} &|M(\mathbf{k}, t_i)|^2 \\ &\quad = \rho_0^2\,|\tilde{f}(\mathbf{k})|^2 - 2\rho_0^2 v \tilde{F}(kR)\mathrm{Re} \\ &\qquad \times \left(\tilde{f}(\mathbf{k}) \sum_{j=1}^{N} e^{-i\cdot\mathbf{k}\cdot\mathbf{r}_j} f(\mathbf{r_j}) \right) + \rho_0^2 v^2 \tilde{F}^2(kR) \\ &\qquad \times \sum_{j=1}^{N}\sum_{i=1}^{N} e^{i\cdot\mathbf{k}\cdot(\mathbf{r}_j-\mathbf{r}_i)} f(\mathbf{r_j}) f(\mathbf{r_i}), \end{aligned} \qquad [15]$$

where Re( ) represents the real part. The first term is the signal of the particle-free liquid. By analogy with the scattering techniques, it corresponds to the nonscattered signal. The second term is called the ''cross term.'' The last term is the important part of the signal, the one that gives information about the internal structure; it is called the ''structure signal.''

The expression Eq. [15] depends on the configuration of the spheres. It appears as a picture of the system. A quantity more adapted to a set of experiments is obtained by averaging Eq. [15] over all possible configurations of particles for the system. This ensemble average is denoted $\langle\ \rangle$ and the mean squared modulus of the magnetization is written as

$$\begin{aligned} &\langle |M(\mathbf{k}, t_i)|^2 \rangle \\ &\quad = \rho_0^2 \cdot |\tilde{f}(\mathbf{k})|^2 - 2\rho_0^2 v \tilde{F}(kR)\mathrm{Re} \\ &\qquad \times \left(\tilde{f}(\mathbf{k}) \left\langle \sum_{j=1}^{N} e^{-i\cdot\mathbf{k}\cdot\mathbf{r_j}} \cdot f(\mathbf{r_j}) \right\rangle \right) + \rho_0^2 v^2 \tilde{F}^2(kR) \\ &\qquad \times \left\langle \sum_{j=1}^{N}\sum_{i=1}^{N} e^{i\cdot\mathbf{k}\cdot(\mathbf{r_j}-\mathbf{r_i})} f(\mathbf{r_j}) f(\mathbf{r_i}) \right\rangle. \end{aligned} \qquad [16]$$

Two different sums of exponentials appear: in the cross term,

$$\left\langle \sum_{j=1}^{N} e^{-i\cdot\mathbf{k}\cdot\mathbf{r_j}} \cdot f(\mathbf{r_j}) \right\rangle, \qquad [17]$$

and another one linked to the structure,

$$\left\langle \sum_{j=1}^{N}\sum_{i=1}^{N} e^{i\cdot\mathbf{k}\cdot(\mathbf{r_j}-\mathbf{r_i})} f(\mathbf{r_j}) f(\mathbf{r_i}) \right\rangle. \qquad [18]$$

In order to calculate the ensemble average in Eq. [17], we introduce the statistical average particle density, denoted $n(\mathbf{r})$:

$$\left\langle \sum_{j=1}^{N} e^{-i\cdot\mathbf{k}\cdot\mathbf{r_j}} \cdot f(\mathbf{r_j}) \right\rangle = \int_E n(\mathbf{r}) f(\mathbf{r}) e^{-i\cdot\mathbf{k}\cdot\mathbf{r}} d\mathbf{r}. \qquad [19]$$

Let us also define

$$m(\mathbf{r}) = n(\mathbf{r})\cdot f(\mathbf{r}) \qquad [20]$$

and its Fourier transform:

$$\tilde{m}(\mathbf{k}) = \int_E m(\mathbf{r}) e^{i\cdot\mathbf{k}\cdot\mathbf{r}} d\mathbf{r}. \qquad [21]$$

In this notation, the ensemble average of the cross term may be written as

$$\mathrm{Mc} = -2\rho_0^2 v \tilde{F}(kR)\mathrm{Re}(\tilde{f}(\mathbf{k})\cdot\tilde{m}^*(\mathbf{k})), \qquad [22]$$

where $\tilde{m}^*(\mathbf{k})$ is the conjugate of $\tilde{m}(\mathbf{k})$.

We have to calculate the ensemble average in Eq. [18], which can be written as a sum of two terms:

$$\begin{aligned} &\left\langle \sum_{j=1}^{N}\sum_{i=1}^{N} e^{i\cdot\mathbf{k}\cdot(\mathbf{r_j}-\mathbf{r_i})} f(\mathbf{r_j}) f(\mathbf{r_i}) \right\rangle \\ &\quad = \left\langle \sum_{i=1}^{N} f(\mathbf{r_i})^2 \right\rangle + \left\langle \sum_{j=1}^{N}\sum_{i\neq j}^{N} e^{i\cdot\mathbf{k}\cdot(\mathbf{r}_j-\mathbf{r_i})} f(\mathbf{r_j}) f(\mathbf{r_i}) \right\rangle. \end{aligned} \qquad [23]$$

Let the two terms on the right-hand side be Ms_1 and Ms_2. The first term is the ensemble average of the function $[f(\mathbf{r})]^2$, which we denote as N,

$$Ms_1 = N, \qquad [24]$$

where

$$N = \int_E [f(\mathbf{r})]^2 n(\mathbf{r}) d\mathbf{r}. \qquad [25]$$

The second term, Ms_2, depends upon the position of two particles. It is then useful to introduce the probability $n(\mathbf{r_1}, \mathbf{r_2}) d\mathbf{r_1} d\mathbf{r_2}$ to find simultaneously a sphere center in the volume $d\mathbf{r_1}$ in the vicinity of position $\mathbf{r_1}$, and another one inside the volume $d\mathbf{r_2}$ in the vicinity of position $\mathbf{r_2}$. The relative

ordering of particles in the suspension is assumed to be sufficiently homogeneous inside the measurement volume (excluding wall effects) for the pair probability density $n(\mathbf{r_1}, \mathbf{r_2})$ to be written as a product of average particle densities at $\mathbf{r_1}$, $\mathbf{r_2}$ and a function depending only on the relative position of the two sphere centers, $\mathbf{r_2} - \mathbf{r_1}$:

$$n(\mathbf{r_1}, \mathbf{r_2}) = n(\mathbf{r_2}) \cdot n(\mathbf{r_1}) \cdot g(\mathbf{r_2} - \mathbf{r_1}). \quad [26]$$

Here, g is the pair distribution function, a fundamental parameter of the internal structure of dispersed media.
Let

$$\mathbf{r_i} = \mathbf{r}'$$
$$\mathbf{r_j} - \mathbf{r_i} = \mathbf{r}. \quad [27]$$

Using Eq. [26] and variables $\mathbf{r}$ and $\mathbf{r}'$, the second term in Eq. [23] becomes

$$Ms_2 = \int_E \int_E e^{i \cdot \mathbf{k} \cdot \mathbf{r}} m(\mathbf{r} + \mathbf{r}') m(\mathbf{r}') g(\mathbf{r}) d\mathbf{r} d\mathbf{r}'. \quad [28]$$

We assume that distant particles are uncorrelated:

$$\lim_{\|\mathbf{r}\| \to \infty} g(\mathbf{r}) = 1. \quad [29]$$

This property leads us to introduce $g(\mathbf{r}) - 1$ in the expression of Ms_2:

$$Ms_2 = \int_E \int_E e^{i \cdot \mathbf{k} \cdot \mathbf{r}} m(\mathbf{r} + \mathbf{r}') m(\mathbf{r}') d\mathbf{r} d\mathbf{r}' + \int_E \int_E \times e^{i \cdot \mathbf{k} \cdot \mathbf{r}} m(\mathbf{r} + \mathbf{r}') m(\mathbf{r}') (g(\mathbf{r}) - 1) d\mathbf{r} d\mathbf{r}'. \quad [30]$$

The first term in the right-hand side is the squared modulus of the Fourier transform of the function $m(\mathbf{r})$. In the second term, we remark the autocorrelation function of $m(\mathbf{r})$ defined as

$$A(\mathbf{r}) = \int_E m(\mathbf{r} + \mathbf{r}') m(\mathbf{r}') d\mathbf{r}'. \quad [31]$$

Finally, the mean structure signal (the last term in Eq. [16]), denoted $M_{St} = \rho_0^2 v^2 \tilde{F}^2(kR)(M_{S1} + M_{S2})$, is written

$$M_{St} = \rho_0^2 v^2 \tilde{F}^2(kR) |\tilde{m}(\mathbf{k})|^2 + \rho_0^2 v^2 \tilde{F}^2(kR) N - \rho_0^2 v^2 \tilde{F}^2(kR) \int_E (1 - g(\mathbf{r})) A(\mathbf{r}) e^{i \cdot \mathbf{k} \cdot \mathbf{r}} d\mathbf{r}. \quad [32]$$

Collecting the averaged cross term Eq. [22] and the structure signal Eq. [32] into Eq. [16], the general expression of the averaged squared modulus of the magnetization becomes

$$\langle |M(\mathbf{k}, t_i)|^2 \rangle = \rho_0^2 \cdot (|\tilde{f}(\mathbf{k})|^2 - 2v\tilde{F}(kR) \mathrm{Re}(\tilde{f}(\mathbf{k}) \cdot \tilde{m}^*(\mathbf{k})) + v^2 \tilde{F}^2(kR) |\tilde{m}(\mathbf{k})|^2) + \rho_0^2 v^2 \tilde{F}^2(kR) \times \left(N - \int_E (1 - g(\mathbf{r})) A(\mathbf{r}) e^{i \cdot \mathbf{k} \cdot \mathbf{r}} d\mathbf{r} \right). \quad [33]$$

This equation can be further reduced to

$$\langle |M(\mathbf{k}, t_i)|^2 \rangle = \rho_0^2 \cdot |(\tilde{f}(\mathbf{k}) - v\tilde{F}(kR) \tilde{m}(\mathbf{k})|^2 + \rho_0^2 v^2 \tilde{F}^2(kR) \times \left(N - \int_E (1 - g(\mathbf{r})) A(\mathbf{r}) e^{i \cdot \mathbf{k} \cdot \mathbf{r}} d\mathbf{r} \right). \quad [34]$$

This result is valid for a suspension of monodisperse spherical beads. We also assumed that the pair probability is of the form of Eq. [26], neglecting the wall effects, and keeping only pair interactions. The analogy with the light scattering is obvious. Since the first term in Eq. [34] is the analogue of the nonscattered rays, we call it the direct signal. The second term is similar to the $I(\mathbf{q})$ intensity function (*2*). In that case $\mathbf{k}$ is simply replaced by $\mathbf{q}$ in the expressions, and the squared form factor $\tilde{F}^2(qR)$ is multiplied by the structure factor $S(\mathbf{q}) = N + \int_E [1 - g(\mathbf{r})] A(\mathbf{r}) e^{i \cdot \mathbf{q} \cdot \mathbf{r}} d\mathbf{r}$. The structure factor denoted $S(\mathbf{q})$ for the scattering techniques and $S(\mathbf{k})$ for the NMR technique describes the microscopic structure through the pair distribution function $g(\mathbf{r})$.

PARTICULAR CASE OF A HOMOGENEOUS SUSPENSION

In order to further simplify the problem, the suspension is now assumed to be homogeneous, that is, the number density of particles in the suspension is constant,

$$n = \frac{N}{V} = \frac{\phi}{v}, \quad [35]$$

where ϕ is the volume fraction.

In this case, $m(\mathbf{r}) = nf(\mathbf{r})$, and Eq. [34] becomes

$$\langle |M(\mathbf{k}, t_i)|^2 \rangle = \rho_0^2 |\tilde{f}(\mathbf{k})|^2 ((1 - \phi \tilde{F}(kR)))^2 + \rho_0^2 v \phi \tilde{F}^2(kR) \times \left(F(\mathbf{0}) - \frac{\phi}{v} \int_E (1 - g(\mathbf{r})) F(\mathbf{r}) e^{i \cdot \mathbf{k} \cdot \mathbf{r}} d\mathbf{r} \right), \quad [36]$$

where $F(\mathbf{r})$ is defined as the autocorrelation function of $f(\mathbf{r})$:

$$F(\mathbf{r}) = \int_E f(\mathbf{r} + \mathbf{r}')f(\mathbf{r}')d\mathbf{r}'. \qquad [37]$$

We already assumed that distant particles are uncorrelated (Eq. [29]). More strictly, we assume here that the correlation length is short compared to the cell dimensions. This is usually the case of settling dilute suspensions of spheres (*12*). It is intuitive that the correlation length decreases with increasing concentration. Thus, in the lack of evidence of the contrary, we also take the assumption that the correlation length is short in a random packing of spheres. Consequently, the integral in Eq. [36] is nonzero in a volume where the function $f(\mathbf{r})$ is constant in a first approximation. Hence, we can write $f(\mathbf{r} + \mathbf{r}') \simeq f(\mathbf{r}')$, and for the autocorrelation function $F(\mathbf{r})$,

$$F(\mathbf{r}) \simeq F(\mathbf{0}). \qquad [38]$$

Finally, we obtain

$$\langle |M(\mathbf{k}, t_i)|^2 \rangle = \rho_0^2 |\tilde{f}(\mathbf{k})|^2 ((1 - \phi\tilde{F}(kR)))^2 + \rho_0^2 v\phi\tilde{F}^2(kR)F(\mathbf{0}) \times \left(1 - \frac{\phi}{v}\int_E (1 - g(\mathbf{r}))e^{i\cdot\mathbf{k}\cdot\mathbf{r}}d\mathbf{r}\right). \qquad [39]$$

As the field gradient **G** is vertical in the experiments, $\mathbf{k}\cdot\mathbf{r}$ is replaced by $k\cdot z$ in Eq. [39].

Consider now the apparatus function $f(\mathbf{r})$. As a first step, let us assume that $f(\mathbf{r})$ is the characteristic function of a cylinder of height h and diameter D, that is, in cylindrical coordinates, $f(z, \rho, \theta)$:

$$\begin{cases} f(z) = 1 & \text{if } -\frac{h}{2} \le z \le \frac{h}{2} \quad \text{and } r \le \frac{D}{2}; \\ f(z) = 0 & \text{if } z > \frac{h}{2} \text{ or } z < -\frac{h}{2} \quad \text{and } r \le \frac{D}{2}. \end{cases} \qquad [40]$$

Then the Fourier transform of $f(\mathbf{r})$ is given by a ''cardinal sine'' function:

$$\tilde{f}(\mathbf{k}) = V\tilde{f}(kh), \qquad [41]$$

where $\tilde{f}(kh) = \mathrm{sinc}(kh/2)$.

The volume V is that of the measurement zone ($V = \pi(D/2)^2h$). Hence, the autocorrelation function $F(\mathbf{0})$ has a simple form:

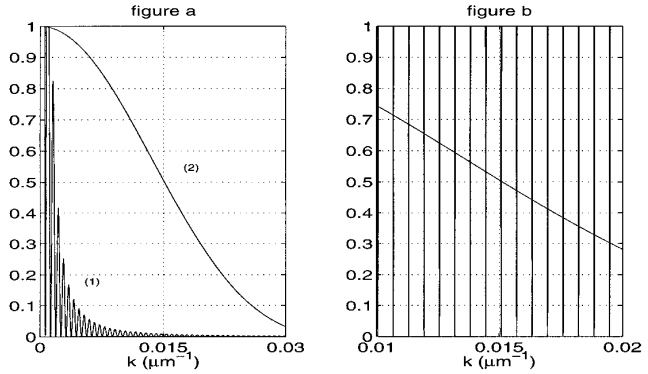

FIG. 3. Comparison between the amplitudes of the direct signal proportional to $\tilde{f}(kh)^2 = \mathrm{sinc}^2(kh/2)$ (*1*), and the structure signal proportional to the squared form factor $\tilde{F}(kR)^2$ (*2*). (a) $\tilde{F}(kR)^2$ and 50 $\mathrm{sinc}^2(kh/2)$. (b) $\tilde{F}(kR)^2$ and 10^5 $\mathrm{sinc}^2(kh/2)$.

$$F(\mathbf{0}) = V. \qquad [42]$$

Equation [39] can be written as

$$\langle |M(k, t_i)|^2 \rangle = \rho_0^2V^2\tilde{f}^2(kh)((1 - \phi\tilde{F}(kR)))^2 + \rho_0^2 vV\phi\tilde{F}^2(kR) \times \left(1 - \frac{\phi}{v}\int_E (1 - g(\mathbf{r}))e^{ikz}d\mathbf{r}\right). \qquad [43]$$

The order of magnitude of the direct signal is $\rho_0^2V^2\tilde{f}^2(kh)$ and that of the structure signal is $\rho_0^2 vV\phi\tilde{F}^2(kR)$. The ratio of the direct signal to the structure signal can then be estimated to be of order $V/v\phi$. For a suspension of spheres of diameter 240 μm with a volume fraction of 10%, in a measurement zone of volume $V = 0.5$ cm^3, this ratio is equal to 7×10^5. Thus, the interesting part of the squared modulus of the magnetization is very small when compared with the peak of the direct signal. Moreover, the Fourier transform of a cylindrical apparatus function is a cardinal sine (Eq. [41]), that is, strongly oscillating. The structure signal is then screened by the oscillations of the direct signal, as shown in Fig. 3. Hence, a ''cylindrical'' apparatus function would not be adapted to the analysis of the structure signal. The actual apparatus function $f(\mathbf{r})$ can be measured by NMR, using the same sequence with a sample of particle-free liquid. The expression for the magnetization then boils down to consider $\phi = 0$ in Eq. [11]:

$$M(\mathbf{k}, t_i) = \rho_0\tilde{f}(\mathbf{k}). \qquad [44]$$

That is, the magnetization is the Fourier transform of $f(\mathbf{r})$ with a multiplicative constant. With the present experimental setup, the apparatus function only varies along the vertical

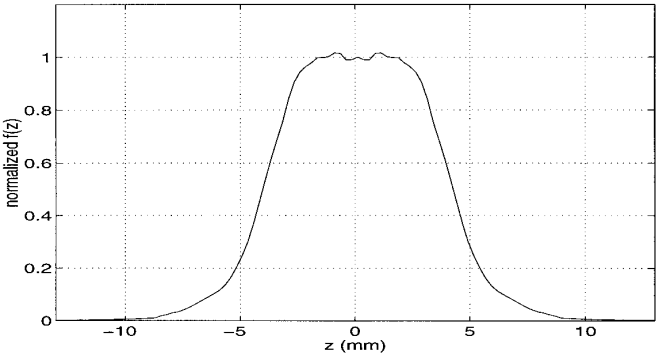

FIG. 4. Experimental result for the apparatus function $f(z)$ which is characteristic of the spatial sensitivity of the detection coil along the z axis. The apparatus function is normalized so that the maximum value is 1.

z and can be described by $f(z)$. The experimental result for $f(z)$ is illustrated in Fig. 4. The general shape is similar to a Gaussian; thus, the Fourier transform $\tilde{f}(k)$ has lower oscillations than the Fourier transform of a cylindrical form and does not screen the structure signal.

We therefore established that the NMR technique using a pulsed field gradient is efficient in the study of dispersed media containing particles embedded in a liquid, such as suspensions. The signal is created by the liquid but gives information about the particles and their configuration. The method consists in following the evolution of the magnetization during the application of a constant gradient field. The squared modulus of the magnetization then depends on microscopic characteristics of the system, such as the mean size of particles and the Fourier transform of the pair distribution function. The expression of the averaged squared modulus of the magnetization is similar to the one of the scattered intensity of the techniques of light, small-angle X-ray scattering, and small-angle neutron scattering, but NMR allows study of systems of larger dimensions.

The classical scattering methods are indeed efficient for particles with a maximum size of 5 μm. For the NMR technique, the range of accessible particle sizes can be estimated as follows. The largest size is fixed by the measurement volume, which corresponds to the range of efficiency of the detection coil. In the experiment, this volume being a cylinder of height $h = 1$ cm, it would be difficult to study systems with a particle size larger than about 1 mm. The smallest size corresponds to the largest wavenumber k in Fourier space, and since $k = \gamma G t$, it corresponds to the largest practically feasible duration t for the NMR sequence. First, the NMR signal decreases because of longitudinal and transverse relaxations (characterized by two relaxation times T_1 and T_2) and heterogeneities of the magnetic field in the measurement zone. In the experiment, the transverse relaxation time T_2^* (which is a combination of T_2 and the effects of heterogeneities of the magnetic field) is about 10 ms. It corresponds to a minimum size of 5 μm. On the other hand, we have assumed until now that the spins in the liquid are fixed during the application of the field gradient (duration t). This hypothesis implies that the movement of the liquid during t is small compared with the diameter of the particles. In particular, the displacement of the liquid due to the thermal agitation must be negligible,

$$\sqrt{2D_0 t} \ll d, \qquad [45]$$

where D_0 is the coefficient of self-diffusion of the water and d is the diameter of the particles. With a maximum duration of 10 ms the condition on the particles diameter is $d > 12$ μm.

In conclusion, the range of accessible sizes by the NMR technique is 10 μm to 1 mm. It completes the range of usual scattering techniques as shown in Fig. 5. This technique is therefore particularly adapted to media with characteristic sizes of about 100 μm, such as suspensions of non-Brownian spheres.

EXPERIMENTAL PROCEDURE AND RESULTS

In order to test the experimental technique, we have chosen to study here packings of hard spheres, then avoiding problems due to the displacement of particles. Note that it would also be possible to study systems in motion such as suspensions or fluidized beds, provided the displacements during the NMR sequence are negligible compared with the diameter of the particles. The particles used are polymer beads of mean diameter 240 μm, and a size standard deviation of 10 μm. The liquid, an alkylbenzyl phthalate, is a plasticizing liquid manufactured by Monsanto. It is appropriate to the study of suspensions because of its large viscosity (1300 times the viscosity of water at 27°C) and its Newtonian behavior when submitted to a weak shear flow. The

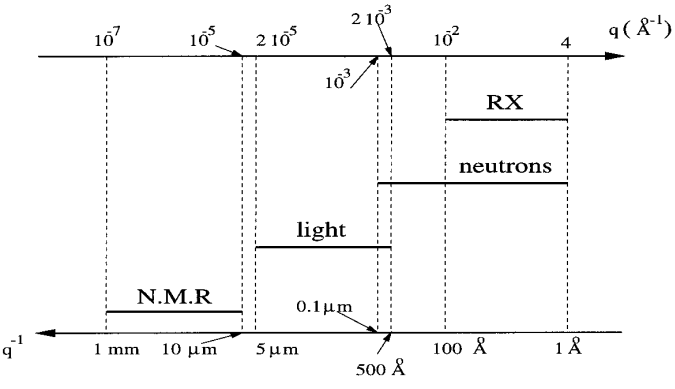

FIG. 5. Range of particle sizes accessible by the NMR technique as compared with the other classical scattering techniques.

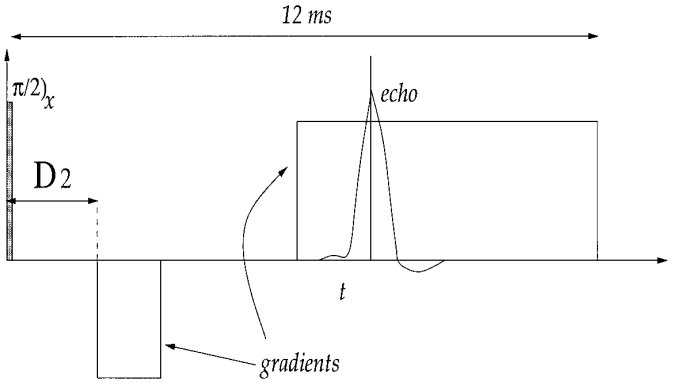

FIG. 6. The gradient echo sequence used in the NMR experiment.

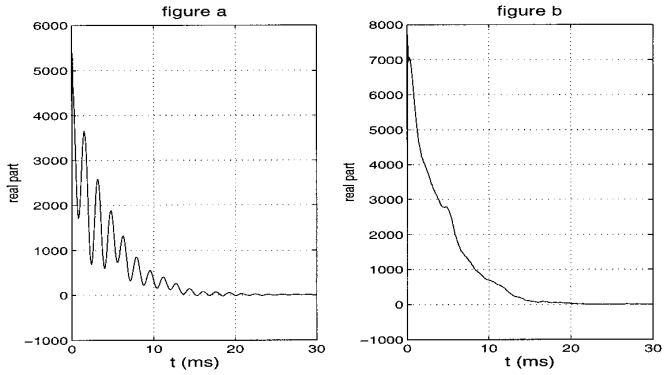

FIG. 7. Free induction decay. The real part of the magnetization obtained without a pulsed field gradient is represented as a function of the time ($k = \gamma \cdot \mathbf{G} \cdot t$). (a) Experimental curve with oscillations. (b) Corrected experimental curve without oscillations.

liquid and beads are in glass tubes of inner diameter 0.8 cm. After mixing with a metallic rod, we wait for 24 h for the spheres to settle to the bottom of the tube. The Stokes sedimentation velocity is here 2.5 $\mu\mathrm{m} \cdot \mathrm{s}^{-1}$.

The pulsed NMR spectrometer is a 100-Mhz Brucker ASX-100. A vertical superconducting coil generates a magnetic field of 2.35 T. A diagram of the spectrometer is shown in Fig. 1. We have already described the detection and gradient coils in the first section. The maximum gradient field is 0.88 T/m, this value being obtained by measuring the molecular diffusion coefficient of water. The NMR sequence is shown in Fig. 6. This is a gradient echo sequence equivalent to the sequence used in the theoretical calculation displayed in Fig. 2. The squared modulus of the magnetization must be averaged over many configurations in order to obtain a significant ensemble average. For that reason, we use several tubes containing the same sediment, and for each tube we measure the magnetization at different vertical positions. As was shown in the first section, the structure signal is 10^6 lower than the direct signal. We therefore accumulate the signal 2000 times, in order to extract the interesting part from the noise.

The free induction decay (FID) shown in Fig. 7a is characterized by a relaxation time T_2^*. The curve oscillates because of the existence of two different resonance frequencies in the NMR spectrum of the liquid. These oscillations are a hindrance for the signal. In order to eliminate them, the same signal is superimposed with a delay corresponding to half a period of the oscillations. This period is 1.6 ms; the duration D_2 (cf Fig. 6) in the second experiment is D_{2in} + 0.8 ms, where D_{2in} is the duration of the first experiment. The result of the superposition (by adjusting a coefficient for minimizing the oscillations) is shown in Fig. 7b. The averaged squared modulus of the magnetization is divided by the corrected FID.

The experimental data for the squared modulus of the magnetization are shown in Fig. 8. Figure 8a displays the curve corresponding to a single configuration, whereas the curve in Fig. 8b corresponding to the accumulation of 20 configurations is an estimate of the ensemble average of the squared modulus of the magnetization. This curve can be interpreted from Eq. [43]. The first term of the expression appears as the largest peak, the base of which is visible in the left-hand side of Fig. 8. This term corresponds to the direct signal. The second term, which depends on the structure of the medium, appears as the remaining part of the curve and is characterized by the second-largest peak. In both graphs, the signal vanishes right after the second peak. This behavior reflects the first zero of the form factor $\tilde{F}(kR)$ (see Fig. 9) which is a multiplicative factor in the structure signal in the second term of Eq. [43]. The zero is obtained for $kR = 4.49$, and we give in Table 1 values of the corresponding modulus of the wave vector **k** for several values of the diameter of the spheres. The actual experimental value is $k = 0.041\ \mu\mathrm{m}^{-1}$, which in Table 1 is associated with a

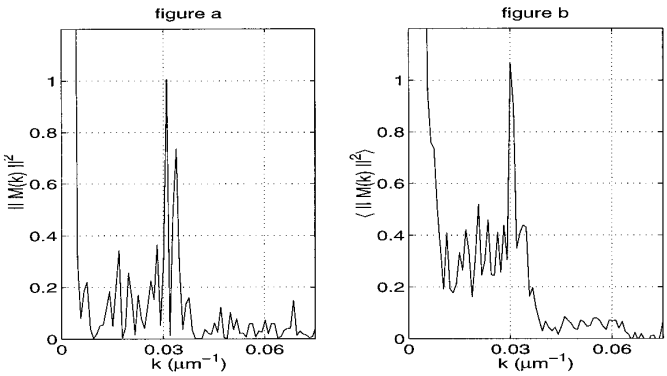

FIG. 8. Experimental results for the squared magnetization modulus. The curves are normalized so that the value of the amplitude of the second largest peak is 1. (a) Typical result using a single configuration in particles. (b) Accumulation over 20 different configurations.

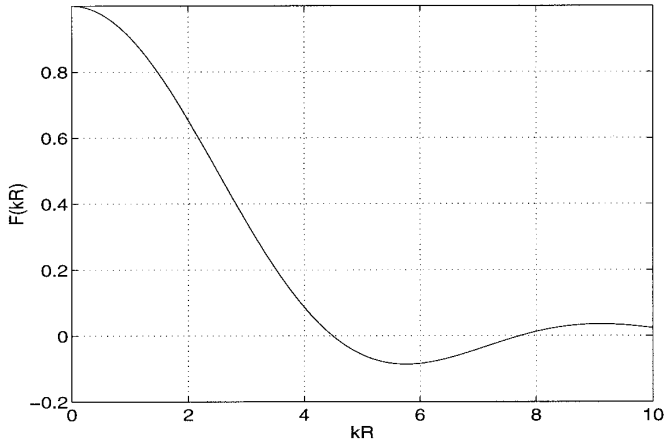

FIG. 9. Form factor $\tilde{F}(kR)$. The first zero occurs for $kR = 4.49$.

diameter of 220 μm. This result is in good agreement with the value of the mean diameter of the sediment (240 μm), the difference being less than 10%. The influence of the particle size polydispersity on the form factor can be taken into account. A Gaussian distribution of sizes with a mean diameter of 240 μm and a standard deviation of 10 μm gives the form factor represented in Fig. 10, this size distribution being a model for the experimental one which is determined by optical microscopy. The amplitude of this function is adapted in order to compare it to the experimental result close to the extinction. In this case, the shape of the form factor approaches the behavior of the experimental curve with a good agreement.

The NMR technique has thus been proved efficient for studying the characteristics of particle size in a suspension. It should be emphasized that the form factor has to be known with good precision, since it multiplies the measured structure factor in the expression of the signal. The influence of the polydispersity may also make the determination of the structure signal difficult. Moreover, we have shown that the signal is related to the pair distribution function. As this pair distribution function may be obtained for an ensemble of spheres by the theory of Percus–Yevick, we now consider the NMR signal corresponding to this model.

PERCUS–YEVICK MODEL FOR THE CALCULATION OF THE SQUARED MODULUS OF THE MAGNETIZATION

An equilibrium distribution of hard spheres is well described by the Percus–Yevick theory, in which only pair interactions are taken into account. The solution of Percus–Yevick is well known, is analytic, and is valid even at high concentrations (*13*).

TABLE 1

Values of the Modulus of the Wave Vector k Corresponding to the First Zero of the Shape Function, for Different Values of the Diameter of the Spheres

Diameter (μm)	200	220	240	260	280
k (μm^{-1})	0.0450	0.0410	0.0375	0.0340	0.031

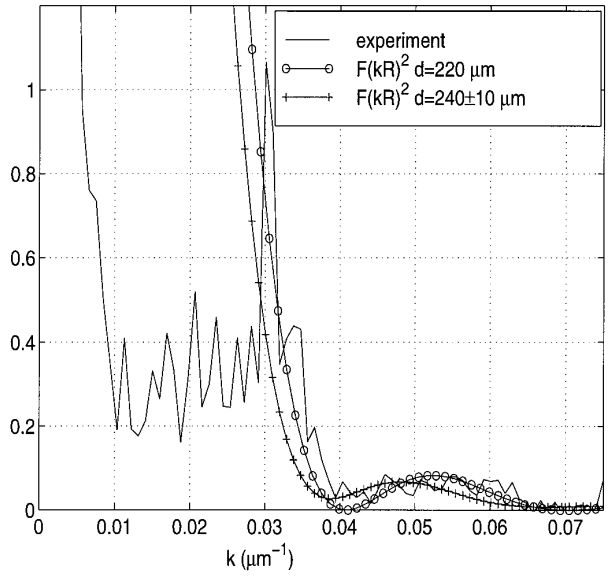

FIG. 10. Comparison between the first extinction of the experimental result with the form factor of particles of diameter 220 μm and the form factor of an ensemble of particles with a Gaussian size distribution $d = 240 \pm 10$ μm. The amplitude of the form factors is adjusted to the experimental curve.

The ensemble average of the squared modulus of the magnetization is given by Eq. [43]. In order to calculate the second term in the right-hand side, that is, the structure signal, the Fourier transform of the function $h(\mathbf{r}) = g(\mathbf{r}) - 1$ must be estimated. $h(\mathbf{r})$ can be simplified by assuming that the pair distribution function does not depend on the direction of the position vector $\mathbf{r}$. The structure signal then becomes

$$M_{st} = \rho_0^2 v V \phi \tilde{F}^2(kR) \left(1 + \frac{\phi}{v}\tilde{h}(k)\right), \qquad [46]$$

in which $\tilde{h}(k)$ is the Fourier transform of $h(r)$. The expression of the function $\tilde{h}(\mathbf{k})$ for an ensemble of hard spheres using the Percus–Yevick approximation is given by Mandel *et al.* (*14*). The analytical formulae are recalled in the Appendix.

The squared modulus of the magnetization has been calculated for volume fractions ranging from 5% to 55%. The results are shown in Fig. 11. The curves are characterized by a large peak. The amplitude of this peak increases with the concentration, and its position is proportional to $\phi^{1/3}$. The experimental compacity of the packing is measured by NMR. The magnetic signal obtained immediately after tilting

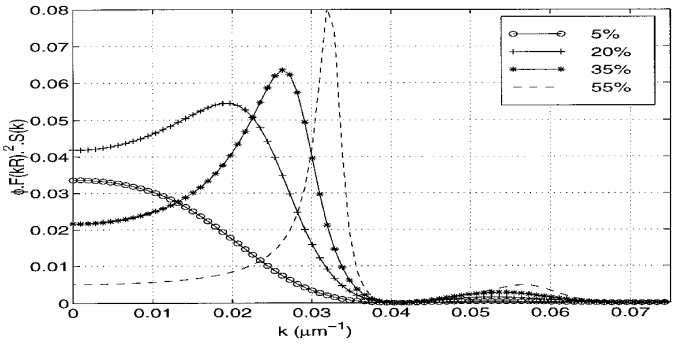

FIG. 11. The Percus–Yevick model. The structure signal $\phi F(kR)^2 S(k)$ for suspensions of different concentrations of particles from 5% to 55% is represented as a function of the modulus of the wave vector $k = \gamma Gt$. $F(kR)$ is the form factor of an ensemble of spheres of diameter 220 μm.

the magnetization onto the horizontal plane is proportional to the number of spins located in the measurement volume. Measuring the signal for the packings and dividing it by the signal generated by the liquid free of particles then provides the compactness of the sediment. The experimental value is 0.56 ± 0.01. The experimental data for the ensemble average of the squared modulus of the magnetization are compared to the results calculated from the Percus–Yevick theory using the experimental volume fraction of particles in Fig. 12. The general shape of both curves is similar. More precisely, the position of the experimental peak corresponds to the modeled one from Percus–Yevick theory when the calculation is made with a volume fraction of 0.57 ± 0.01. This value is in good agreement with the experimental compacity of 0.56.

In conclusion, the Percus–Yevick theory thus gives a good description of the experimental squared modulus of the magnetization. However, this description is not comprehensive: First, it only takes into account pair interactions. Second, since the positions of the spheres in the settling sediment depend on the many-particle hydrodynamic interactions during all preceding phases of sedimentation, the resulting configurations should be in principle different from the ones in a completely random model.

A fully comprehensive model of the settling sediment should take into account the many-particle hydrodynamic interactions (*15*) together with the interactions with the walls, which is not yet achieved.

CONCLUSION

We have developed a novel NMR technique particularly adapted to the study of the structure of systems of particles in a liquid. The modulus of the magnetization due to the protons of the liquid (with particles containing no proton) is calculated in the presence of a constant pulsed field gradient and then averaged over all possible configurations accessible to the particles. The suspension is assumed to be homogenous, and in order to simplify the interpretation of the result we considered spherical particles of the same size. The averaged squared modulus of the magnetization obtained in this case is related to the pair distribution function of the particles $g(\mathbf{r})$ (see [43]). This expression is analogous to the one that gives the scattered intensity $I(\mathbf{q})$ in the classical scattering techniques (X-rays, light, neutrons) as a function of the wave vector $\mathbf{q}$. In the present NMR technique, the wave vector denoted $\mathbf{k}$ is given by $\mathbf{k} = \gamma \mathbf{G} t$, where γ is the gyromagnetic ratio, $\mathbf{G}$ the intensity of the pulsed field gradient, and t the duration of application of this gradient. The exploration of the $\mathbf{k}$-space is thus obtained by simply measuring the magnetization as a function of time. As in the classical expression of $I(\mathbf{q})$, the structure factor $S(\mathbf{k})$ defined as the Fourier transform of $1 - g(\mathbf{r})$ appears multiplied by $\tilde{F}^2(kR)$, where $\tilde{F}(kR)$ is the form factor, the Fourier transform of a function characteristic of the shape of the particles. The first term in the expression [43] contains $\tilde{f}(kh)$, the Fourier transform of the apparatus function which describes the sensitivity of the detection coil of the spectrometer and defines the measurement zone. This term, which corresponds to the nonscattered rays in the classical scattering techniques, is usually omitted. For the NMR technique, however, we show that the apparatus function can screen the interesting part of the signal if its shape is not adapted.

The range of particles sizes accessible by the NMR technique is 10 μm to 1 mm. It thus completes the range of the classical scattering techniques, which is 0.5 Å to 5 μm.

The technique is validated by studying packings of spheres of mean diameter 240 μm. The spheres are embedded in a liquid rich in protons and packings are obtained by sedimentation of the particles. In the case of the scattering techniques, the number of particles is sufficiently important and

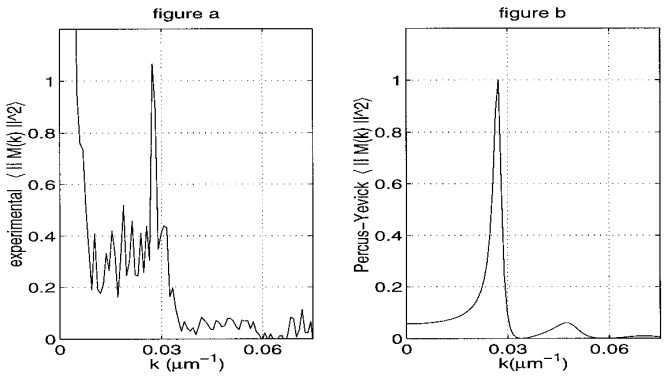

FIG. 12. Ensemble average of the squared modulus of the magnetization: comparison between the experimental curve (a) and the model using Percus–Yevick approximation with a volumic fraction of 56% (b). The curves are adjusted so the amplitude of the peak is equal to 1.

a single measurement gives an averaged value. In this experiment, however, we have to cumulate the results for a number of different packings in order to average the squared modulus of the magnetization. The general shape for the experimental data of the averaged squared modulus of the magnetization depends on the pair distribution function. It is found to be in good agreement with a model based on the Percus–Yevick approximation. We also obtain the mean diameter and the compactness of the packings from the experiments, and in this way confirm the validity of the NMR technique.

These results are an incentive to study various other systems with particles of sizes ranging from 10 μm to 1 mm, such as non-Brownian suspensions, fluidized beds, and porous media. In the case of suspensions and fluidized beds, the particles are in motion, and the necessary condition for using NMR is that the displacement of the particles during the NMR sequence be small compared to their diameter. If this condition is verified, the averaged squared modulus of the magnetization gives information about the pair distribution function which depends on the hydrodynamic interactions between particles. There is a lack of theory for this dependence in inhomogenous and/or concentrated suspensions. This technique should thus provide determinant information for the development of a more realistic model of suspensions.

APPENDIX: CALCULATION OF THE FOURIER TRANSFORM OF $h(r)$

Let us define λ_1 and λ_2:

$$\begin{cases} \lambda_1 = \dfrac{(1+2\phi)^2}{(1-\phi)^4} \\ \lambda_2 = -\dfrac{(1+0.5\phi)^2}{(1-\phi)^4}, \end{cases}$$

where ϕ is the volume fraction in particles.

The Fourier transform of the function $h(r)$, denoted $\tilde{h}(k)$, is given by

$$\tilde{h}(k) = \frac{\tilde{c}(k)}{1 - n_0\tilde{c}(k)}, \qquad [48]$$

where $\tilde{c}(k)$, the Fourier transform of the indirect correlation function $c(r)$, may be expanded as

$$\tilde{c}(k) = d^3(\tilde{c}_1(kd) + \tilde{c}_2(kd) + \tilde{c}_3(kd)), \qquad [49]$$

in which

$$\begin{cases} \tilde{c}_1(kd) = \left[-\dfrac{4\pi\lambda_1}{(kd)^3}\right][\sin(kd) - kd\cos(kd)] \\ \tilde{c}_2(kd) = \left[-\dfrac{24\pi\lambda_2}{(kd)^4}\right][2kd\sin(kd) \\ \qquad - ((kd)^2 - 2)\cos(kd) - 2] \\ \tilde{c}_3(kd) = \left[-\dfrac{2\pi\lambda_1}{(kd)^6}\right]\{[-(kd)^4 + 12(kd)^2 - 24] \\ \qquad \times \cos(kd) + [4(kd)^3 - 24kd] \\ \qquad \times \sin(kd) + 24\}. \end{cases} \qquad [50]$$

Here d is the diameter of the particles, and $n = 6\phi/\pi d^3$.

REFERENCES

1. I. R. Hansen and I. R. McDonald, ''Theory of Simple Liquids,'' Academic Press, London, 1976.
2. B. J. Berne and R. Pecora, ''Dynamic Light Scattering,'' Wiley, New York, 1976.
3. A. Guinier and G. Fournet, ''Small Angle Scattering of X-Rays,'' Wiley, New York, 1955.
4. E. O. Stejskal, *J. Chem. Phys.* **43,** 3597 (1965).
5. K. Fukuda and A. Hirai, *J. Phys. Soc. Jap.* **47,** 1999 (1979).
6. J. Kärger and W. Heink, *J. Magn. Reson.* **51,** 1 (1983).
7. P. Mansfield and P. K. Grannel, *Phys. Rev. B* **12,** 3618–3634 (1975).
8. P. T. Callaghan, D. MacGowan, K. J. Packer, and F. O. Zelaya, *J. Magn. Reson.* **90,** 177 (1990).
9. D. G. Cory and N. Garroway, *Magn. Res. Med.* **14,** 435 (1990).
10. P. T. Callaghan, A. Coy, D. MacGowan, K. J. Packer, and F. O. Zelaya, *Nature* **351,** 467 (1991).
11. G. A. Barral, L. Frydman, and G. C. Chingas, *Science* **255,** 714 (1992).
12. G. K. Batchelor and C. S. Wen, *J. Fluid Mech.* **124,** 495 (1982).
13. W. R. Smith and D. Henderson, *Mol. Phys.* **19,** 411 (1970).
14. F. Mandel, R. J. Bearman, and M. Y. Bearman, *J. Chem. Phys.* **57**(7), 3315 (1970).
15. B. Cichocki, B. U. Felderhof, K. Hinsen, E. Wajnryb, and J. Blawzdziewicz, *J. Chem. Phys.* **100,** 3780 (1994).